Supplementary Information

Table of Content:

Supplementary Figure 1

A

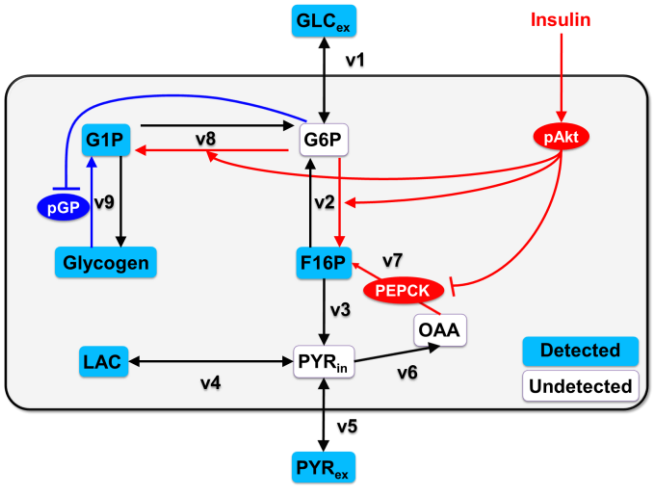

B

Re. ID	Reaction name	Reaction	V_1	K_1	V_2	K_2	Pram. ID
v1	Glucose transport	$GLC_{ex} \underset{V_2,K_2}{\overset{V_1,K_1}{\rightleftarrows}} G6P$	8.9698278	0.0450710	-	-	1, 2
v2	Mutual conversion of G6P and F16P	$G6P \underset{V_2,K_2}{\overset{V_1,K_1}{\rightleftarrows}} F16P$	7.7110234	924.95773	0.0838920	0.5974682	3, 4, 5, 6
v3	Conversion of F16P to PYR$_{in}$	$F16P \xrightarrow{V_1,K_1} PYR_{in}$	0.0022883	2.9169988	-	-	7, 8
v4	Mutual conversion of PYR$_{in}$ and LAC	$PYR_{in} \underset{V_2,K_2}{\overset{V_1,K_1}{\rightleftarrows}} LAC$	23.636950	56.430376	0.0000012	0.0154094	9, 10, 11,12
v5	Pyruvate transport	$PYR_{ex} \underset{V_2,K_2}{\overset{V_1,K_1}{\rightleftarrows}} PYR_{in}$	0.0011242	0.2277173	-	-	13, 14
v6	Conversion of PYR$_{in}$ to OAA	$PYR_{in} \xrightarrow{V_1,K_1} OAA$	0.0024697	0.9964752	-	-	15, 16
v7	Conversion of OAA to F16P	$OAA \xrightarrow{V_1,K_1} F16P$	0.0000284	8.4278976	-	-	17, 18
v8	Mutual conversion of G6P and G1P	$G6P \underset{V_2,K_2}{\overset{V_1,K_1}{\rightleftarrows}} G1P$	0.0000202	0.7911906	0.0399818	69.846920	19, 20, 21, 22
v9	Mutual conversion of G1P and glycogen	$G1P \underset{V_2,K_2}{\overset{V_1,K_1}{\rightleftarrows}} Glycogen$	0.4877346	2.6908550	0.0000010	0.0006233	23, 24, 25, 26
v10	Allosteric regulation of pGP by G6P	$GP \underset{V_2}{\overset{V_1}{\rightleftarrows}} pGP + G6P$	112.75732	-	1.9447813	-	27, 28
v11	Phosphorylation of FoxO1 by pAKT	$pAKT + FoxO1 \underset{V_2}{\overset{V_1}{\rightleftarrows}} pFoxO1$ (active) (inactive)	0.1222521	-	0.0045984	-	29, 30
v12	mRNA regulation of PEPCK by FoxO1	$\xrightarrow[\downarrow V_1]{FoxO1\ (active)} mRNA_{PEPCK} \xrightarrow[V_2]{} \phi$	486.28471	-	0.0046101	-	31, 32
v13	Protein synthesis of PEPCK	$\xrightarrow{V_1} Protein_{PEPCK} \xrightarrow[V_2]{} \phi$	0.0001095	--	0.0018592	-	33, 34

C

Initial amounts

Molecular Name	Initial value	Pram. ID
GLC_{ex}	114.9 (μM)	-
G6P	0.5188 (μM)	35
F16P	9.571 (μM)	-
PYR_{in}	0.9872 (μM)	36
LAC	1001 (μM)	-
G1P	5.303 (μM)	-
Glycogen	1 (A.U.)	-
OAA	0.0022 (μM)	37
PYR_{ex}	137.5 (μM)	-
GP	0.4726 (A.U.)	38
pGP	0.1723 (A.U.)	-
FoxO1	$1.069x10^{-5}$ (A.U.)	39
pFoxO1	0 (A.U.)	-
$mRNA_{PEPCK}$	$2.905x10^{-4}$ (A.U.)	40
PEPCK	0.7686 (A.U.)	41

D

Scale factors

Scale Factor	Reaction	value	Pram. ID
s_1	G6P to F16P by pAKT	1.722	42
s_2	OAA to F16P by PEPCK	46.54	43
s_3	G6P to G1P by pAKT	1.190	44
s_4	Glycogen to G1P by pGP	214.7	45

E

Rate equations

$$v_1 = \frac{V_{1\_v1}\frac{[GLC_{ex}]}{K_{1\_v1}} - V_{1\_v1}\frac{[G6P]}{K_{1\_v1}}}{1+\frac{[GLC_{ex}]}{K_{1\_v1}}+\frac{[G6P]}{K_{1\_v1}}}$$

$$v_2 = \frac{\left(1+s_1\cdot[pAKT]\right)V_{1\_v2}\frac{[G6P]}{K_{1\_v2}} - V_{2\_v2}\frac{[F16P]}{K_{2\_v2}}}{1+\frac{[G6P]}{K_{1\_v2}}+\frac{[F16P]}{K_{2\_v2}}}$$

$$v_3 = \frac{V_{1\_v3}[F16P]}{K_{1\_v3}+[F16P]}$$

$$v_4 = \frac{V_{1\_v4}\frac{[PYR_{in}]}{K_{1\_v4}} - V_{2\_v4}\frac{[LAC]}{K_{2\_v4}}}{1+\frac{[PYR_{in}]}{K_{1\_v4}}+\frac{[LAC]}{K_{2\_v4}}}$$

$$v_5 = \frac{V_{1\_v5}\frac{[PYR_{ex}]}{K_{1\_v5}} - V_{1\_v5}\frac{[PYR_{in}]}{K_{1\_v5}}}{1+\frac{[PYR_{ex}]}{K_{1\_v5}}+\frac{[PYR_{in}]}{K_{1\_v5}}}$$

$$v_6 = \frac{V_{1\_v6}[PYR_{in}]}{K_{1\_v6}+[PYR_{in}]}$$

$$v_7 = \frac{\left(1+s_2\cdot[PEPCK]\right)V_{1\_v7}[OAA]}{K_{1\_v7}+[OAA]}$$

$$v_8 = \frac{\left(1+s_3\cdot[pAKT]\right)V_{1\_v8}\frac{[G6P]}{K_{1\_v8}} - V_{2\_v8}\frac{[G1P]}{K_{2\_v8}}}{1+\frac{[G6P]}{K_{1\_v8}}+\frac{[G1P]}{K_{2\_v8}}}$$

$$v_9 = \frac{V_{1\_v9}\frac{[G1P]}{K_{1\_v9}} - \left(1+s_4\cdot[pGP]\right)\cdot V_{2\_v9}\frac{[Glycogen]}{K_{2\_v9}}}{1+\frac{[G1P]}{K_{1\_v9}}+\frac{[Glycogen]}{K_{2\_v9}}}$$

$$v_{10} = V_{1\_v10}[GP] - V_{2\_v10}[pGP][G6P]$$

$$v_{11} = V_{1\_v11}[FoxO1][pAKT] - V_{2\_v11}[pFoxO1]$$

$$v_{12} = V_{1\_v12}[FoxO1] - V_{2\_v12}[mRNA_{PEPCK}]$$

$$v_{13} = V_{1\_v13}[mRNA_{PEPCK}] - V_{2\_v13}[Protein_{PEPCK}]$$

F

ODEs

$$V_{ex}\cdot\frac{d[GLC_{ex}]}{dt} = -v_1$$

$$V_{in}\cdot\frac{d[G6P]}{dt} = v_1 - v_2 - v_8$$

$$V_{in}\cdot\frac{d[F16P]}{dt} = v_2 - v_3 + v_7$$

$$V_{in}\cdot\frac{d[PYR_{in}]}{dt} = v_3 - v_6 - v_4 + v_5$$

$$V_{in}\cdot\frac{d[LAC]}{dt} = v_4$$

$$V_{in}\cdot\frac{d[G1P]}{dt} = v_8 - v_9$$

$$V_{in}\cdot\frac{d[Glycogen]}{dt} = v_9$$

$$V_{in}\cdot\frac{d[OAA]}{dt} = v_6 - v_7$$

$$V_{ex}\cdot\frac{d[PYR_{ex}]}{dt} = -v_5$$

$$\frac{d[GP]}{dt} = -v_{10}$$

$$\frac{d[pGP]}{dt} = v_{10}$$

$$\frac{d[FoxO1]}{dt} = -v_{11}$$

$$\frac{d[pFoxO1]}{dt} = v_{11}$$

$$\frac{d[mRNA_{PEPCK}]}{dt} = v_{12}$$

$$\frac{d[Protein_{PEPCK}]}{dt} = v_{13}$$

G Volume factors

Volume name	value
V_{ex}: Extracellular volume	4.00×10^{-3} Litter
V_{in}: Intracellular volume	2.64×10^{-5} Litter

H Parameter values for the insulin-dependent AKT pathway model

Pram. ID	Parameter value
P1	5.5702
P2	2.3969
P3	2.0934×10^{-2}
P4	1.2140×10^{-5}
P5	2.7510×10^{-1}
P6	7.2509×10^{-3}
P7	7.5812×10^{2}
P8	9.1758×10^{-1}
P9	4.1292×10^{-2}
P10	1.3032×10^{-4}
P11	1.9200×10^{-4}
P12	2.9311×10^{-2}
P13	4.4307×10^{-5}
P14	3.5211×10^{-1}
P15	8.8877×10^{2}
P16	1.1182
P17	3.1385×10^{-5}
P18	9.5934×10^{-3}
P23	8.8025×10^{2}

Supplementary Figure 1. The insulin-dependent glucose metabolism model.

(A) Block diagram of the AKT-dependent glucose metabolism model. The designations v1 through v9 are the reaction IDs (Supplementary Figure 1B). The red lines indicate metabolic reactions that are regulated by the insulin-dependent AKT pathway, whereas the blue line indicates the G6P-induced allosteric effect of pGP. The insulin-dependent glucose metabolism model consists of two sub-models, the insulin-dependent AKT pathway model and the AKT-dependent glucose metabolism model. In this study, we newly developed the AKT-dependent glucose metabolism model based on Michaelis-Menten kinetics for the metabolic reactions and mass action kinetics for the G6P-induced phosphorylation of GP and the pAKT-induced gene expression of PEPCK. We also used Michaelis-Menten kinetics for glucose transport because GLUT2, which is the major glucose transporter expressed in hepatocytes, mediates the facilitated diffusion of glucose in an insulin-independent manner (Tirone & Brunicardi, 2001). We used "The insulin to AKT module" in the previously developed insulin-dependent AKT pathway model for the upstream pAKT signalling pathway; the detailed reactions and ordinary differential equations used in this sub-model were as previously described (Kubota et al, 2012), and the re-estimated parameters for the insulin-dependent AKT pathway model are shown in Supplementary Figure 1H. **(B)** Reactions and parameters of the AKT-dependent glucose metabolism model. "Re. ID" indicates the reaction IDs, which correspond to "v#" in Supplementary Figure 1A. "Param. ID" indicates the parameter IDs. **(C)** Initial amounts of the molecules used in the AKT-dependent glucose metabolism model. **(D)** Scale factors of the

reactions used in the AKT-dependent glucose metabolism model. **(E) (F)** Ordinary differential equations used in the AKT-dependent glucose metabolism model. The effect of pAKT on the regulation of the metabolic enzymes was implemented by changing V_{max} of the reaction rates (Mosca et al, 2012). The simulations were performed using MATLAB (see also Materials and Methods). **(G)** Extracellular and intracellular volumes in the ODEs. Extracellular volume corresponds to the volume of media in the experiments, and intracellular volume were estimated (Le Cam & Freychet, 1977) (see also Materials and Methods). **(H)** The parameter values for the insulin-dependent AKT pathway model re-estimated in the current study (see also Materials and Methods). The parameter IDs P1 to P18 and P23 correspond to those in the previous study (Kubota et al, 2012).

Supplementary Figure 2

A

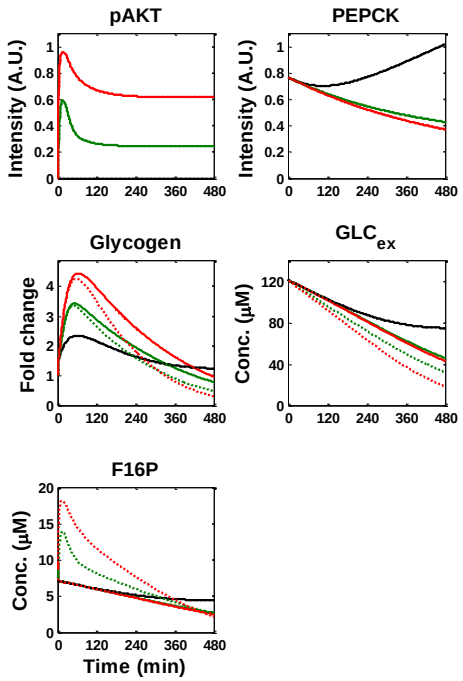

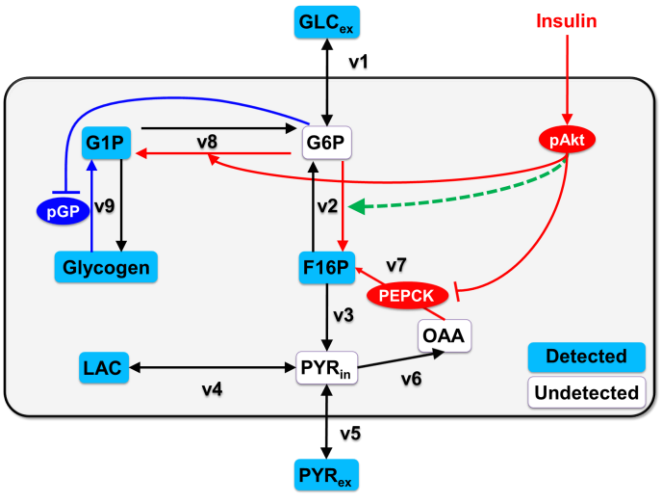

B

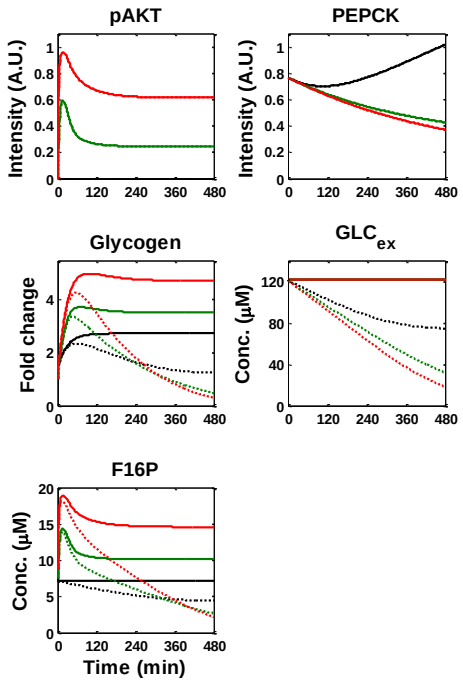

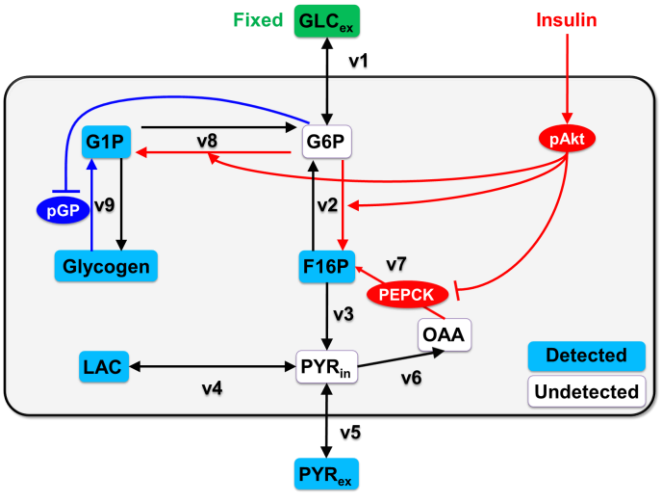

C

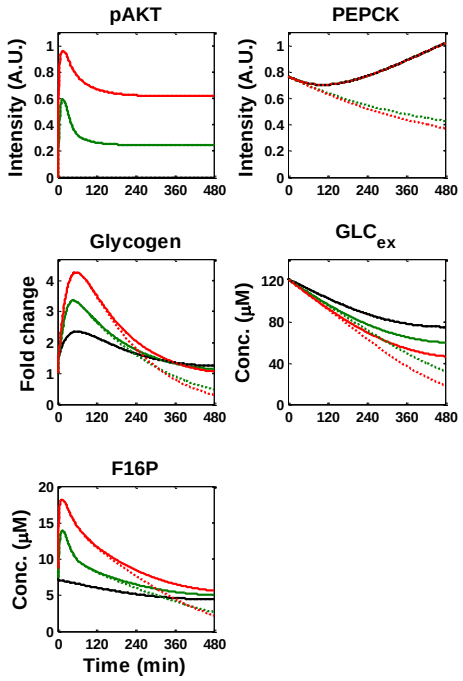
pAKT
PEPCK
Intensity (A.U.)
Glycogen
GLC$_{ex}$
Fold change
Conc. (μM)
F16P
Conc. (μM)
Time (min)

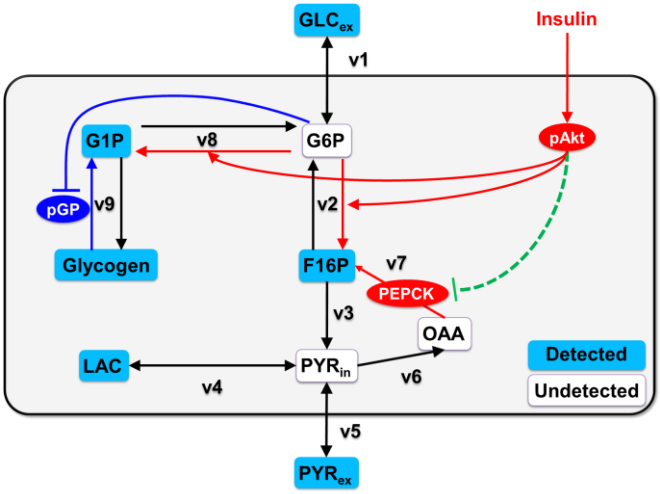
GLC$_{ex}$
Insulin
v1
G1P
v8
G6P
pAkt
pGP
v9
v2
Glycogen
F16P
v7
PEPCK
v3
OAA
LAC
PYR$_{in}$
v6
v4
Detected
Undetected
v5
PYR$_{ex}$

D

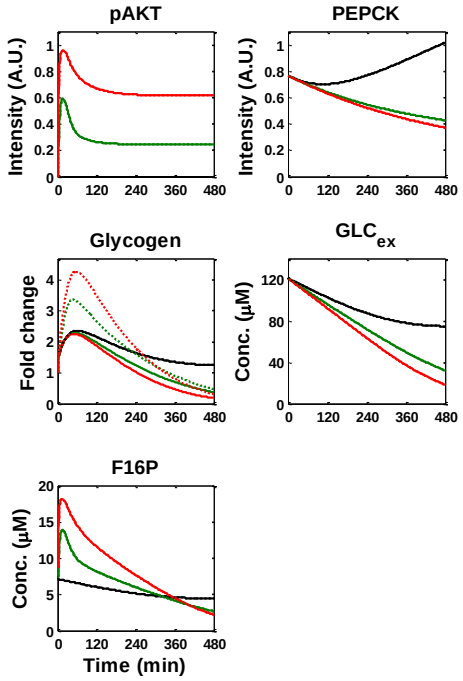
pAKT
PEPCK
Intensity (A.U.)
Glycogen
GLC$_{ex}$
Fold change
Conc. (μM)
F16P
Conc. (μM)
Time (min)

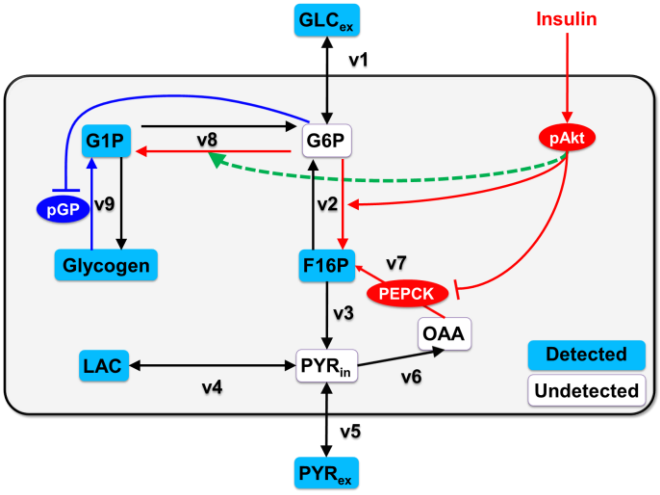
GLC$_{ex}$
Insulin
v1
G1P
v8
G6P
pAkt
pGP
v9
v2
Glycogen
F16P
v7
PEPCK
v3
OAA
LAC
PYR$_{in}$
v6
v4
Detected
Undetected
v5
PYR$_{ex}$

E

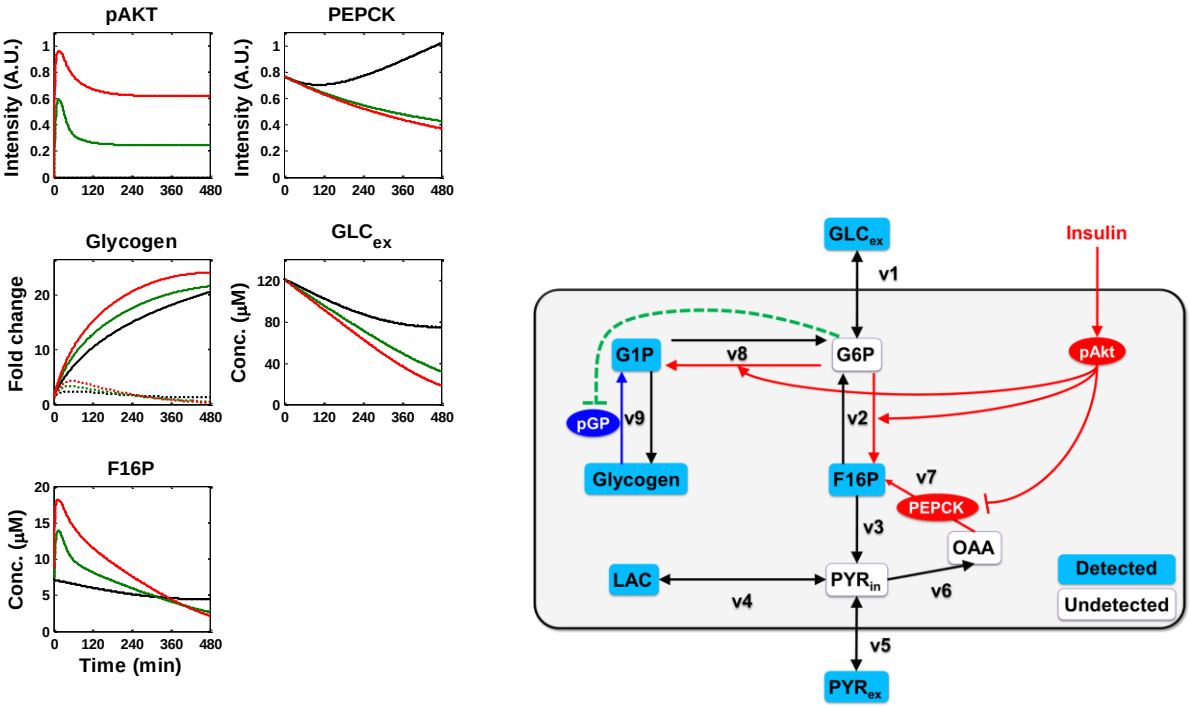
pAKT
PEPCK
Intensity (A.U.)
Glycogen
GLC$_{ex}$
Fold change
Conc. (μM)
F16P
Conc. (μM)
Time (min)
GLC$_{ex}$
Insulin
v1
G1P
v8
G6P
pAkt
pGP
v9
v2
Glycogen
F16P
v7
PEPCK
v3
OAA
LAC
PYR$_{in}$
v6
v4
Detected
Undetected
v5
PYR$_{ex}$

F

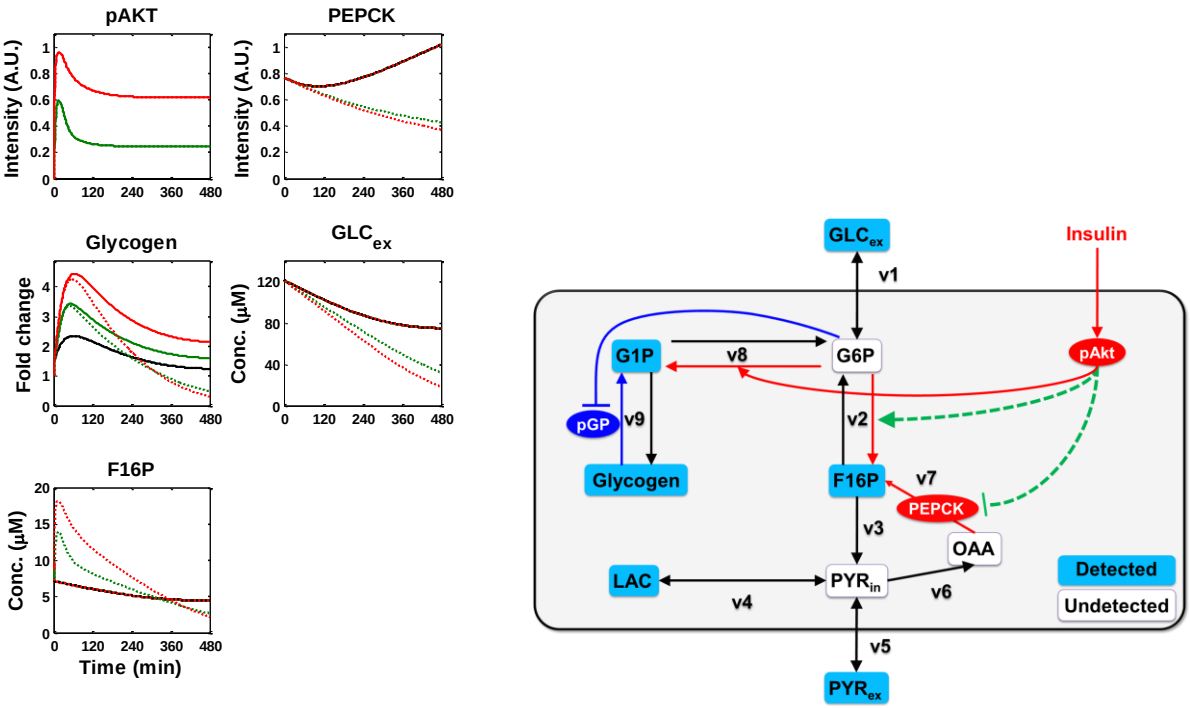
pAKT
PEPCK
Intensity (A.U.)
Glycogen
GLC$_{ex}$
Fold change
Conc. (μM)
F16P
Conc. (μM)
Time (min)
GLC$_{ex}$
Insulin
v1
G1P
v8
G6P
pAkt
pGP
v9
v2
Glycogen
F16P
v7
PEPCK
v3
OAA
LAC
PYR$_{in}$
v6
v4
Detected
Undetected
v5
PYR$_{ex}$

Supplementary Figure 2. Specific deletion of reactions in the insulin-dependent pathway.

(A) Deletion of the pAKT-mediated conversion of G6P to F16P. Deletion of the pAKT-to-F16P pathway resulted in the disappearance of the transient increase of F16P, indicating that the direct regulation of F16P by pAKT was responsible for the transient increase of F16P. **(B)** Insulin-dependent responses of pAKT, F16P, PEPCK, glycogen, GLC_{ex} and pGP with constant GLC_{ex} (which was maintained at its initial concentration). The maintenance of GLC_{ex} prevented the decrease of F16P, indicating that the substrate depletion of extracellular glucose is responsible for the decrease of F16P. **(C)** Deletion of the AKT-dependent suppression of PEPCK. Deletion of the pAKT-to-PEPCK pathway prevented the sustained decrease of PEPCK, indicating that the regulation of PEPCK by pAKT was responsible for the sustained decrease of PEPCK. **(D)** Deletion of the pAKT-dependent production of G1P. Deletion of the pAKT-to-G1P pathway prevented the transient increase of glycogen, indicating that the pAKT-to-G1P pathway is responsible for the transient increase of glycogen. **(E)** Deletion of the G6P-dependent inhibition of pGP prevented the decrease of glycogen, indicating that pGP is responsible for the adaptive response of glycogen. **(F)** Deletion of the pAKT-mediated conversion of G6P to F16P and the pAKT-dependent suppression of PEPCK prevented the decrease of GLC_{ex} that is observed in response to insulin, indicating that, in this model, GLC_{ex} is regulated by gluconeogenesis and glycolysis, but not by glycogenesis. Green dotted lines in the right block diagrams represent the deleted pathway. The black, green and red lines indicate the

various insulin concentrations used (0, 1 and 100 nM, respectively), and the solid and dotted lines indicate the time courses obtained with each specific deletion model and with the intact model (control, Figure 2A), respectively.

Supplementary Figure 3

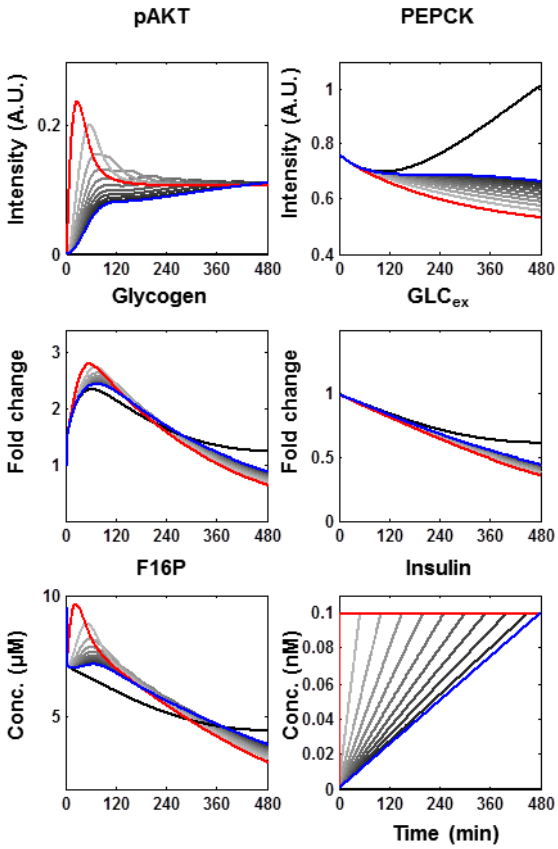

Supplementary Figure 3. The sensitivity of F16P, PEPCK, glycogen and GLC_{ex} to the rate of insulin increase.

Responses of pAKT, F16P, PEPCK, glycogen and GLC_{ex} to the rate of insulin increase. These responses were obtained using the simulation model. The rates of insulin increase are indicated using colours. Black lines indicate the responses of the molecules without stimulation of insulin, and blue lines and red lines indicate the responses of the molecules to the ramp stimulation and the step stimulation, respectively, which are corresponds to Figure 4.

Supplementary Figure 4

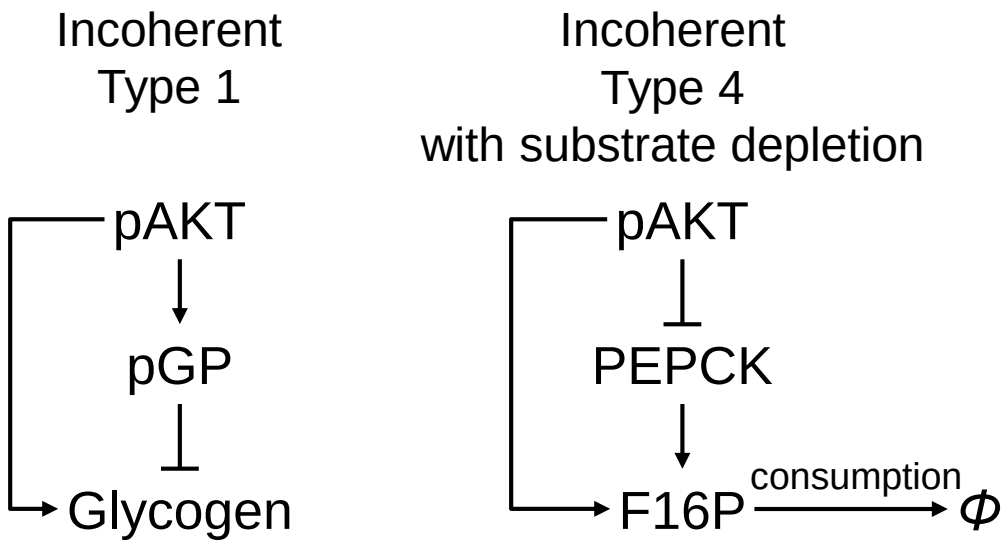

Supplementary Figure 4. The structure types of incoherent feedforward loops.

There are four structure types of incoherent feedforward loops (Mangan & Alon, 2003). In this study, we reveal that the network structure of glycogen regulation by insulin via pAKT forms an Incoherent Type 1 and that of the 3-node network of pAKT, PEPCK and F16P forms an Incoherent Type 4 with substrate depletion. Note that in our model, the transient response of F16P is mainly generated by an increase via feedforward by pAKT and a decrease due to substrate depletion, rather than the negative regulation via PEPCK (see also Supplementary Figure 2C).

Supplementary Figure 5

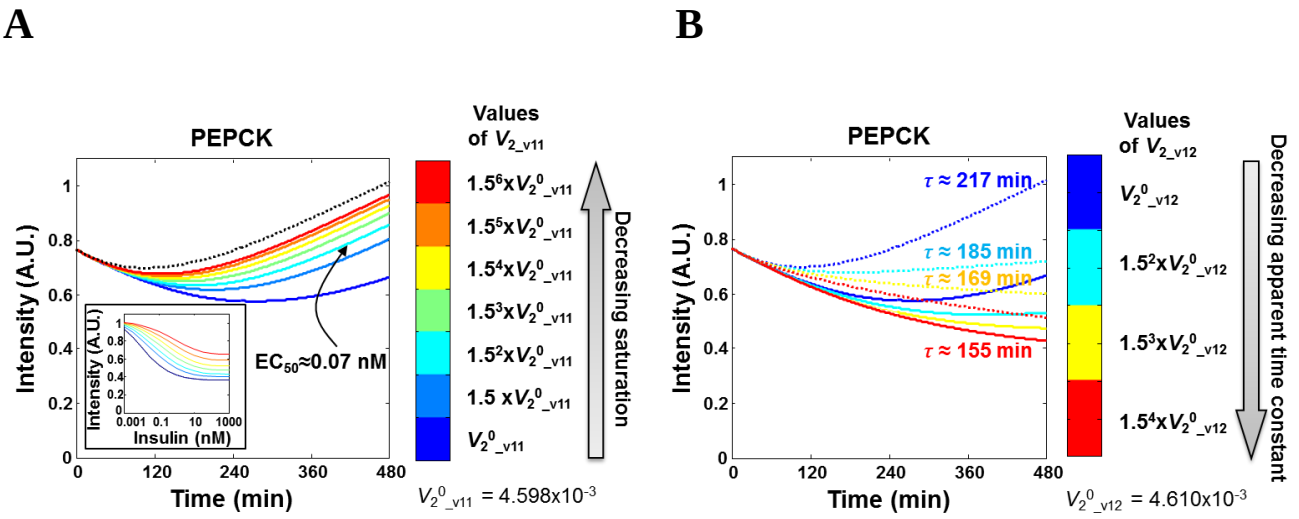

Supplementary Figure 5. The effect of decreasing the saturation or apparent time constant on the responsiveness of PEPCK to an insulin pulse stimulation.

(A) The effect of saturation on the responsiveness of PEPCK to an insulin pulse stimulation. The saturation was decreased by increasing the EC_{50} through increasing the V_{2_v11} of "Phosphorylation of FoxO1 by pAKT" (Supplementary Figure 1B, Re. ID: v11, Param. ID: 30). Ten-min pulse stimulation was used, and black dotted line indicates the basal level. The colour bar indicates the values of V_{2_v11}. The inset represents dose-response curves of PEPCK against various concentrations of insulin with the different values of V_{2_v11}, and the line colours of the dose-response curves correspond to those of the time courses. EC_{50} became larger as line colours turned from blue to red. The EC_{50} of PEPCK with 1.5^2 x $V_2{}^0{}_{\_v11}$ (cyan line) were calculated to be approximately 0.07 nM from the inset, which corresponds to that of *G6Pase* in the previous study (Kubota et al, 2012). **(B)** The effects of the apparent time constant on the responsiveness of PEPCK to an insulin pulse

stimulation. The apparent time constant was decreased by increasing the V_{2_v12} of “mRNA regulation of PEPCK by FoxO1” (Supplementary Figure 1B, Re. ID: v12, Param. ID: 32). Dotted lines indicate each basal level. The colour bar indicates the values of V_2. The indicated values “τ” represent each apparent time constant with the different values of V_{2_v12}, and the font colours correspond to the line colours. The apparent time constants became smaller as line colours turned from blue to red. We computationally calculated the apparent time constants, which is the time required for the response to reach 63.2% of the final value, from Supplementary Figure 5B. The apparent time constant of *G6Pase* were 18 min (Kubota et al, 2012).

Supplementary References

Kubota H, Noguchi R, Toyoshima Y, Ozaki Y, Uda S, Watanabe K, Ogawa W, Kuroda S (2012) Temporal coding of insulin action through multiplexing of the AKT pathway. *Molecular cell* **46:** 820-832

Le Cam A, Freychet P (1977) Neutral amino acid transport. Characterization of the A and L systems in isolated rat hepatocytes. *The Journal of biological chemistry* **252:** 148-156

Mangan S, Alon U (2003) Structure and function of the feed-forward loop network motif. *Proceedings of the National Academy of Sciences of the United States of America* **100:** 11980-11985

Mosca E, Barcella M, Alfieri R, Bevilacqua A, Canti G, Milanesi L (2012) Systems biology of the metabolic network regulated by the Akt pathway. *Biotechnology advances* **30:** 131-141

Tirone TA, Brunicardi FC (2001) Overview of glucose regulation. *World journal of surgery* **25:** 461-467